action of electrons and phonons. Note that the last term of (2.7b) usually does not appear.

3. The adiabatic approximation overestimates the kinetic energy, while static approach overestimates the potential energy.

4. Electron transitions affect the equilibrium positions of the ions and the frequency of the normal modes. One cannot, in general, justify the consideration of these effects independently.

5. The splitting of the Hamiltonian leads to several mathematical difficulties. The static approximation gives non-orthogonal wave functions while the adiabatic gives non-Hermitian operators.

6. The adiabatic approach is superior for deeper traps. A rough estimate indicates that it should be used when the binding energy is greater than 0.1 ev.

7. For very shallow traps the static approach may be superior at low temperatures. Actually, the difference between the two for depths of about 0.1 ev or less is so small that there is little choice, and other approximations made in a calculation will be of greater importance.

ACKNOWLEDGMENTS

The author would like to acknowledge some very helpful discussions with his colleagues. Particular mention should be made of Professor F. Seitz, who read the first draft, Dr. P. Clavier, who suggested some of the proofs in Sec. 2, and Dr. H. J. G. Meyer of Eindhoven for valuable criticism. The assistance of Mrs. M. Parker with the calculation and of Mrs. H. Pietrini with the manuscript is also gratefully acknowledged.

PHYSICAL REVIEW VOLUME 103, NUMBER 3 AUGUST 1, 1956

Radio-Frequency Spectra of Li^6Cl by the Molecular Beam Electric Resonance Method*

D. T. F. MARPLE† AND J. W. TRISCHKA
Syracuse University, Syracuse, New York

(Received January 16, 1956)

Transitions between the hyperfine structure levels of the rotational state of Li^6Cl with $J=1$ were studied by the molecular beam electric resonance method. The electric quadrupole interaction constant, $(eqQ)_{Cl}$, and the spin-rotation interaction constant, c_{Cl}, of the chlorine nucleus, and the product of the square of the molecular dipole moment, μ^2, and moment of inertia, A, were determined in several different vibrational states. These constants, and the ratios derived from them are:

for Li^6Cl^{35}	$v=0$	$v=1$	$v=2$	$v=3$
$(eqQ/h)_{Cl}$ (kc/sec)	-3071.72 ± 0.61	-3479.3 ± 1.7	-3873.0 ± 1.8	-4250 ± 11
c/h_{Cl} (kc/sec)	2.07 ± 0.10	2.22 ± 0.20	2.19 ± 0.21	···
μ^2A ($\times10^{76}$ cgs)	1774.26 ± 0.28	1840.26 ± 0.40	1909.3 ± 0.6	1980.6 ± 0.9
for Li^6Cl^{37}				
$(eqQ/h)_{Cl}$ (kc/sec)	-2419.9 ± 2.4	-2736.6 ± 5.4	···	···
c/h_{Cl} (kc/sec)	1.88 ± 0.30	1.60 ± 0.34	···	···
μ^2A ($\times10^{76}$ cgs)	1788.24 ± 0.40	1854.9 ± 0.6	1924.7 ± 0.7	···
$(eqQ)_{Cl^{35}}/(eqQ)_{Cl^{37}}$	1.2694 ± 0.0013	1.2714 ± 0.0025	···	···
$\mu^2A(Li^6Cl^{37})/\mu^2A(Li^6Cl^{35})$	1.00788 ± 0.00027	1.0081 ± 0.001	···	···

The random errors in μ^2A are given in the foregoing. The systematic error was $\pm1.1\times10^{-76}$ cgs.

The vibrational constant, ω_e, was found to be 536 ± 60 cm^{-1} from a study of line intensities. The magnetic field at the chlorine nucleus, H_R, was calculated to be 4.96 ± 0.23 gauss from c_{Cl} for Li^6Cl^{35} in the zeroth vibrational state. μ, and the internuclear distance, r, were found from beam deflection data to be 5.9 ± 1.3 Debye units 2.4 ± 0.4 A, respectively.

A static electric field was used to study the Stark effect. When the static field was weak or absent, line frequencies were found to depend on the magnitude of the radio-frequency field used to produce transitions. This effect is termed "radio-frequency Stark effect." A theory for this effect was developed and accounts for the observations.

INTRODUCTION

RADIO-FREQUENCY spectra of Li^6Cl^{35} and Li^6Cl^{37} were studied by the molecular beam electric resonance method.[1–3] Transitions were induced between the electric hyperfine structure levels of the rotational state with $J=1$ by an oscillating field applied in the region between two inhomogeneous fields which selected the initial and final states to be observed. Stark effect was produced by a static electric field superimposed on the oscillating field.

Two nuclear-molecular interactions, the electric quadrupole interaction and the spin-rotation interaction of the Cl nuclei, were required to explain the observed spectra. The product of the square of the molecular

* This work was supported in part by the Office of Naval Research. Reproduction in whole or in part is permitted for any purpose of the United States Government.

† Present address: General Electric Research Laboratory, Schenectady, New York.

[1] H. K. Hughes, Phys. Rev. **72**, 614 (1947).
[2] J. W. Trischka, Phys. Rev. **74**, 718 (1948).
[3] Lee, Fabricand, Carlson, and Rabi, Phys. Rev. **91**, 1395 (1953).

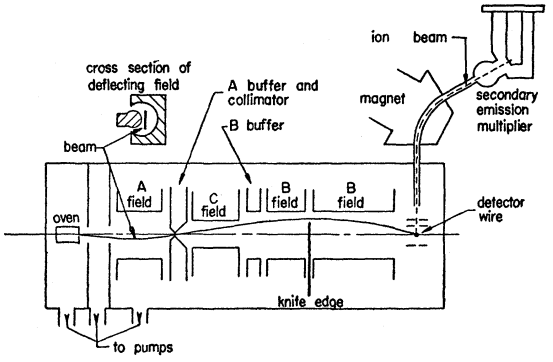

FIG. 1. Schematic diagram of the apparatus.

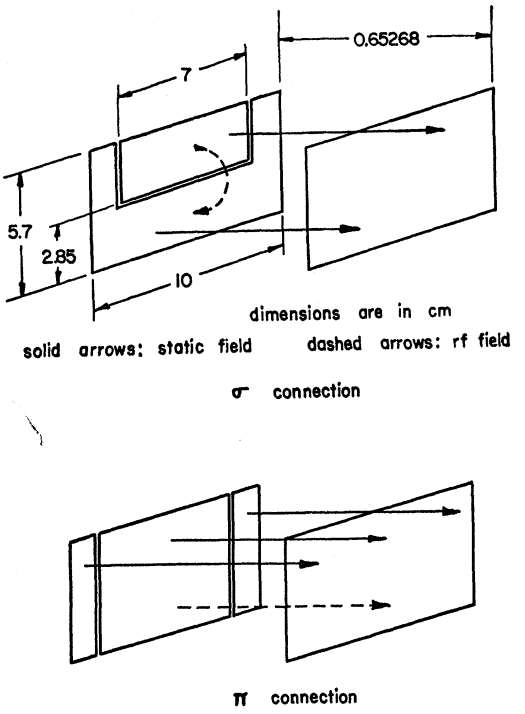

FIG. 2. Schematic diagram of the C-field electrode configurations and fields with the π and σ connections.

dipole moment and the moment of inertia was determined from spectra observed with a large static field. The interaction constants were determined for several different vibrational states. The absolute variation of the chlorine quadrupole interaction with vibration was the largest yet observed in any alkali chloride. Because of this variation, spectra of each vibrational state of each isotopic species could be observed separately even at zero static field.

When the static field was small or absent, shifts in line frequencies were observed which in all cases depended quadratically on the radio-frequency field strength. This effect will be referred to as "radio-frequency Stark effect" because the effect on the observed spectra was similar to that produced by a static field. Similar effects have been observed in microwave spectra[4] but have not been previously reported in electric resonance experiments. The theory used to explain earlier electric resonance experiments[5,6] does not predict any dependence of transition frequencies on radio-frequency field strength. Since the present results could not be accounted for as an apparatus defect, the theory was re-examined. A new theory, developed below, agrees with the results used to explain the microwave observations and accounts for the present observations.

APPARATUS AND BEAM INTENSITIES

Figure 1 is a schematic diagram of the electric resonance apparatus. The details and dimensions of the different parts have been described before.[7–9] In operation, a beam of LiCl molecules from the heated oven passed through the first inhomogeneous field, A, the collimator slit, the C-field, and the second inhomogeneous field, B, to a hot wire detector. The detector dissociated the molecules and produced Li ions. About 60% of the Li^6 ions could be directed by a gun through the mass spectrometer. Ion currents from the mass spectrometer were measured either with an electrometer amplifier[10] or with a secondary emission multiplier which was added to the apparatus for the present experiments. The multiplier was based on the Allen[11] design, used heat-activated brass dynodes, and gave a multiplication of 2.1×10^5 for 5-kv Li ions. No drop in multiplication was found after the dynodes were exposed to the atmosphere for more than 400 hours. Details of the construction and performance of the multiplier have been given previously by one of the authors.[12] The ion currents could be measured with the multiplier much more rapidly, and for currents of 10^{-14} amp or less, with much better signal-to-noise ratio than with the electrometer amplifier.

The beam was deflected in the inhomogeneous fields because of the interaction between the field gradient and the average dipole moment induced by the field. The deflections depended on the rotational quantum number, J, the space quantization, specified by the component of J in the field direction, m_J, and the field strength. For the present experiments, the inhomogeneous fields were adjusted so that molecules in the state $J=1$, $m_J=1$ in the A-field, [hereafter abbreviated $(1,1)_A$], were deflected in the B-field to reach the detector if they were in the state $(1,0)_B$; thus transitions produced in the C-field were observed as increases in the beam strength at the detector. When resonances

[4] C. H. Townes and F. R. Merritt, Phys. Rev. **72**, 1266 (1947).
[5] H. C. Torrey, Phys. Rev. **59**, 293 (1941).
[6] V. Hughes and L. Grabner, Phys. Rev. **79**, 819 (1950).
[7] R. G. Luce and J. W. Trischka, J. Chem. Phys. **21**, 105 (1953).
[8] J. C. Swartz and J. W. Trischka, Phys. Rev. **88**, 1085 (1952).
[9] R. Braunstein and J. W. Trischka, Phys. Rev. **98**, 1092 (1955).
[10] D. B. Pennick, Rev. Sci. Instr. **6**, 115 (1935).
[11] J. S. Allen, Rev. Sci. Instr. **18**, 739 (1947).
[12] D. T. F. Marple, Rev. Sci. Instr. **26**, 1205 (1955).

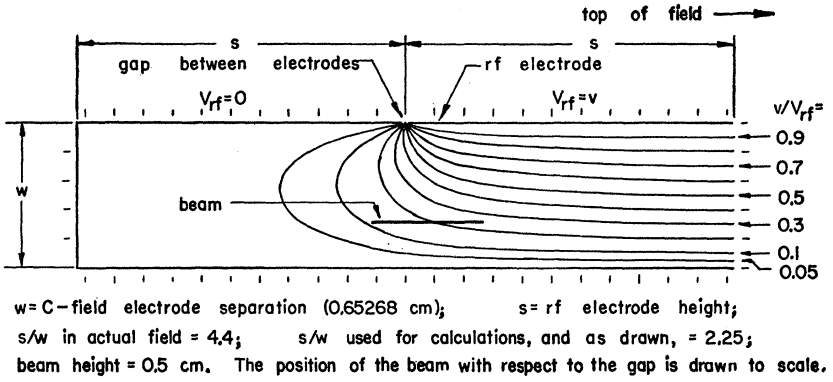

FIG. 3. Equipotential lines of the rf field, calculated for the plane perpendicular to the electrodes and equidistant from their ends, with the σ connection of the electrodes.

were studied, a knife edge was arranged to obstruct the direct path between the oven and the detector. The knife-edge prevented molecules which were only slightly deflected (those in high J states) from reaching the detector. Buffer fields were used to make the change in field strength between the inhomogeneous fields and the relatively weak C-field less abrupt. They helped to preserve the space quantization through the interfield regions.

The ion current measured with the knife-edge removed and no fields applied gave a measure of the total beam intensity. This current was 6×10^{-11} amp at an oven temperature of 805°K and 1×10^{-11} amp at 740°K. A typical value was 2×10^{-11} amp and the other observed ion currents given below have been adjusted to correspond to this value.

When the knife edge was inserted but no fields were applied, scattered molecules reached the detector. This scattered beam gave an ion current of 3×10^{-16} amp. When the A- and B-fields were applied, the beam strength at the detector increased even though no radio-frequency field was applied in the C-field. This increase will be called the residual beam. At zero static C-field a typical residual beam gave an ion current of 4×10^{-15} amp, and was one tenth as large with the C-field at 200 v/cm or greater.

With the A- and B-fields adjusted to study $(1,1)_A$–$(1,0)_B$ transitions as described above, the change in the ion current from the detector produced when the strength of a buffer field was reduced to zero gave a useful check on operating conditions during a run. With the C-field at 200 v/cm or larger, a typical "refocused beam" was 4×10^{-15} amp, about 10% as great as the ion current expected if all the $(1,1)_A$ molecules made a transition to the $(1,0)_B$ state.

The most intense spectral lines gave an ion current change of 1×10^{-15} amp, and were observed with a signal-to-noise ratio of about 50 against a steady background of 1×10^{-15} amp. The least intense lines gave an ion current change of about 5×10^{-17} amp and a signal-to-noise ratio of about 4.

Two different connections of the C-field electrodes were used and are shown in Fig. 2. The static field distribution was the same in both connections, but the strengths of the radio-frequency field parallel and perpendicular to the static field, the π and σ components, respectively, depended on the connection. In the π connection, the oscillating field had no σ component except near the ends of the C-field, and the field strength in the central region could be calculated easily from the electrode spacing and applied voltage. Both π and σ components were present when the σ connection was used, and the strength of both components in the central region was needed for the analysis of the radio-frequency Stark effect observations. To obtain these field strengths, a "grid" of potentials at different points in the field was calculated by a relaxation method.[13] To shorten these calculations, the approximate configuration shown in Fig. 3 was used instead of the dimensions in Fig. 2. The equipotential lines, shown in Fig. 3, were obtained by interpolation between the calculated points. The measured position of the beam in the field is also shown in Fig. 3. The intensities of the π and σ components at the beam position are shown in Fig. 4 as a function of the distance above and below the center of the beam.

THEORY

The theory will be developed in two parts. First, the important features of the predicted Li^6Cl spectra as they appear with static fields of different strengths will be developed from the general expressions for the energy levels and selection rules given by Hughes and Grabner,[6] Bardeen and Townes,[14] and Fano.[15] Second, a theory of the radio-frequency Stark effect will be developed in general and applied to specific cases.

The complete Hamiltonian[6,14] includes the interaction of the molecular electric dipole moment, μ, with the electric field, the nuclear electric quadrupole interactions of the Li and Cl nuclei, characterized by the interaction constants $(eqQ)_{Li}$ and $(eqQ)_{Cl}$, respectively, and the spin-rotation interactions, $(c\mathbf{I}\cdot\mathbf{J})$, of the two

[13] V. E. Cosslett, *Introduction to Electron Optics* (Clarendon Press, Oxford, 1946), p. 22.
[14] J. Bardeen and C. H. Townes, Phys. Rev. **73**, 97 (1948).
[15] U. Fano, J. Research Natl. Bur. Standards **40**, 215 (1948).

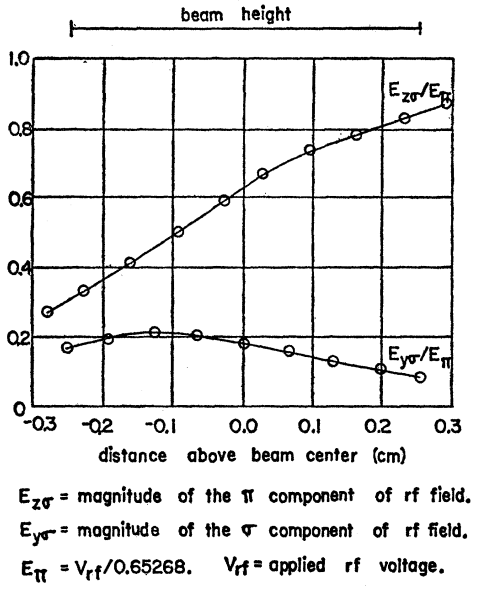

FIG. 4. Radio-frequency fields at the beam position with the σ connection of the electrodes.

nuclei, characterized by the constants c_{Li} and c_{Cl}. The nuclear magnetic dipole-dipole interaction is also included, and is characterized by the interaction constant $g_1g_2\mu_N^2/r^3$, where g_1g_2 is the product of the nuclear gyromagnetic ratios, μ_N is one nuclear magneton, and r is the internuclear distance.

Estimates of the Li interaction constants could be made from past observations. The magnitude of $(eqQ)_{\mathrm{Li}^7}$,[16] was used with the ratio $Q_{\mathrm{Li}^6}/Q_{\mathrm{Li}^7}$,[17] to calculate $(eqQ)_{\mathrm{Li}^6}/h=4.24$ kc/sec. The width of the Li^6 central resonance in the $\mathrm{Li}^6\mathrm{Cl}$ magnetic resonance spectrum[18] was treated as entirely due to the Li spin-rotation interaction and analyzed with the methods given by Nierenberg and Ramsey[19] to give $c_{\mathrm{Li}}/h=0.19$ kc/sec. With $r=1.97$ A,[20] $g_1g_2\mu_N^2/r^3h=0.23$ kc/sec for Cl^{35}.

The energy levels in the absence of a static field were calculated with the methods and matrix elements developed by Bardeen and Townes.[14] The ratio $(eqQ)_{\mathrm{Cl}}/(eqQ)_{\mathrm{Li}}$ is so large that the splittings due to the Li interactions could be calculated separately from those due to Cl. All of the line frequency calculations given below refer to transitions from the state $(1,1)_A$ to the state $(1,0)_B$. At zero field, spectra may be observed only by the two-quantum process.[6] In the present experiments, the two quanta were of the same frequency so that the observed lines appeared at exactly half the frequencies given by the theory outlined above. These are called "half-frequency" lines. When the Li and magnetic dipole-dipole interactions were neglected, application of the selection rules and observability criterion[6] showed that three lines should appear if $(eqQ)_{\mathrm{Cl}}$ is negative and that the low-frequency line should be absent if $(eqQ)_{\mathrm{Cl}}$ is positive. If all the interactions are included, each line is split up into a group of closely spaced lines. Within each group, the predicted lines are so closely and symmetrically spaced that no resolved structure and no shift in the mean frequency of the lines is greater than the experimental error in the measurements unless the lines farthest from the mean position are much more intense than the others. As this is not very likely, the Li and magnetic dipole-dipole interactions have been ignored in the analysis of the spectra. A more refined calculation could be made if the strength of individual lines in a group could be reliably calculated. Since these strengths depend on the distribution of the nonadiabatic transitions in the interfield regions, the intensity calculation could not be made without knowledge of the field strengths in the interfield regions, which are not known.

If $(eqQ)_{\mathrm{Cl}}$ changes appreciably with vibrational state, groups of two, or three, lines will appear [depending on the sign of $(eqQ)_{\mathrm{Cl}}$], where each group is produced by molecules in a different vibrational state. The intensity of corresponding lines in these groups is proportional to the population of the vibrational states in the beam.

In all the weak field observations, the static field was so large that the Stark effect was much bigger than the splittings due to the Li or magnetic dipole-dipole interactions. With the estimated interaction constants given above, and the matrix elements calculated in a suitable representation,[6] it was found that these interactions could also be neglected at weak fields.

The spectra predicted by the weak-field approximation[6] and selection rules when only the Cl interactions and Stark effect are included are shown in Fig. 5 for the case $(eqQ)_{\mathrm{Cl}}<0$ and $c_{\mathrm{Li}}>0$. Both full- and half-frequency lines may be observed at weak field, and the selection rules for transitions produced by the π component of the oscillating field differ from those for the σ component or for the two-quantum combinations. The different cases are included in Fig. 5, and it will be noted that the Stark effect is different in the various cases.

At strong fields, the energy level splittings due to the static field are much greater than those due to any internal interactions in the molecule. The strong-field approximation[6] may then be used, and when only the Cl interactions are included this theory predicts six lines[21] spaced symmetrically about a center frequency. The separation of the six lines depends only on $(eqQ)_{\mathrm{Cl}}$

[16] Logan, Coté, and Kusch, Phys. Rev. **86**, 267 (1952).
[17] N. A. Schuster and G. E. Pake, Phys. Rev. **81**, 157 (1951).
[18] P. Kusch, Phys. Rev. **75**, 887 (1949).
[19] W. A. Nierenberg and N. F. Ramsey, Phys. Rev. **72**, 1075 (1947).
[20] E. S. Rittner, J. Chem. Phys. **19**, 1030 (1951).

[21] V. Hughes and L. Grabner, reference 6. The following errors have been found: Fig. 2 (p. 820), line 4 does not appear at strong fields; Fig. 3 (p. 821), line 4 does not appear at strong fields; Fig. 8 (p. 824), Stark line does not appear in (2,0–2,2) spectra. The outermost lines do not appear in (2,1–2,2) spectra. None of these errors affects the conclusions in their paper.

and c_{Cl}, and the center frequency is determined by $\mu^2 A$, where A is the moment of inertia of the molecule.

At intermediate fields, the perturbations in the energy caused by the static field are the same order of magnitude as the splittings due to the internal interactions. The energy levels were calculated with Fano's[15] methods, modified to include the matrix elements of the Cl spin-rotation interaction. Energy levels calculated with this theory are correct at all fields, and the weak field selection rules apply at all intermediate fields. The spectrum for each isotopic species and vibrational state consists of seven lines, and the position of one line with respect to the others depends directly on the sign of $(eqQ)_{Cl}$. Thus the sign of $(eqQ)_{Cl}$ may be determined entirely from the line frequencies in an intermediate field spectrum. This determination is entirely independent of the observability criterion which may be violated under zero or weak field conditions because of the nonadiabatic transitions in the interfield regions.

For the purposes of the present experiment it is also useful to distinguish a strong-intermediate field region. Here the strong-field selection rules apply and the qualitative features of the spectrum are the same as with a strong field. The energy levels are not given with sufficient accuracy by the strong-field approximation, and the intermediate-field theory must be used. However, the line separations depend only very slightly on the field strength and the center frequency only very slightly on the internal interactions. This case will be needed later in the analysis of the observations.

Since $\mu^2 A$, $(eqQ)_{Cl}$ and c_{Cl} change with vibrational state several groups of six or seven lines are expected at strong and intermediate fields, respectively. The intensities of corresponding members of these groups should be proportional to the population of the vibrational states in the beam.

Some qualitative features of the radio-frequency Stark effect have already been discussed in the introduction. A detailed outline of a theory for this effect developed by one of us (DTFM) is given below.

The time-dependent Schrödinger equation is taken as

$$H(t)\psi = i\hbar(\partial\psi/\partial t), \tag{1}$$

and the true wave function is expanded as

$$\Psi = \sum_n a(n,t)u(n,t)\exp\left[-i/\hbar\int_{t_0}^{t} E(n,t')dt'\right], \tag{2}$$

where the functions $u(n,t)$ are determined from

$$H(t)u(n,t) = E(n,t)u(n,t). \tag{3}$$

Equation (2) is substituted into (1). It may be shown[22,23] that the equations for the $a(n)$ then are

$$\dot{a}(k) = \sum_n \frac{a(n)}{\hbar\omega_{kn}}\left\langle k\left|\frac{\partial H}{\partial t}\right|n\right\rangle \exp\left[-\int_{t_0}^{t}\omega_{kn}(t')dt'\right], \tag{4}$$

where

$$\omega_{kn} = [E(k,t) - E(n,t)]/\hbar.$$

Following Schiff,[24] $H(t)$ and $a(n)$ are expressed as

$$H(t) = H_0 + \lambda H'(t),$$

where $\lambda H'(t) \ll H_0$,

$$a(n) = \sum_s \lambda^s a(n)^{(s)}, \tag{5}$$

and are substituted into (4). When equal powers of λ are equated,

$$a(n)^{(0)} = c,$$

$$\dot{a}(k)^{(s+1)} = \sum_n \frac{a(n)^{(s)}}{\hbar\omega_{kn}}\left\langle k\left|\frac{\partial H'(t)}{\partial t}\right|n\right\rangle \times\exp\left[-i\int_{t_0}^{t}\omega_{kn}(t')dt'\right]. \tag{6}$$

If it is assumed that $a(n) = 1$ at $t = t_0$, when the perturbation is applied, then for a short time afterwards (6) is, for $s = 0$,

$$\dot{a}(k)^{(1)} = \frac{1}{\hbar\omega_{kn}}\left\langle k\left|\frac{\partial H'(t)}{\partial t}\right|n\right\rangle \exp\left[-i\int_{t_0}^{t}\omega_{kn}(t')dt'\right]. \tag{7}$$

Equation (7) is now integrated to obtain the $a(k)^{(1)}$, the first approximations to the true expansion coefficients $a(k)$.

Two cases are of particular interest to the electric resonance experiments with LiCl. In the first case, it is assumed that the molecule is a rigidly rotating dipole and that one nucleus has an electric quadrupole interaction. In the expressions which follow, E_{dc} is the static electric field, E_{rf} is the radio-frequency field with angular frequency ω, H_Q and E_Q are the Hamiltonian and energy for the quadrupole interaction, $E(J)$ is the rotational energy, and $d(F,m_F)$ are coefficients given by

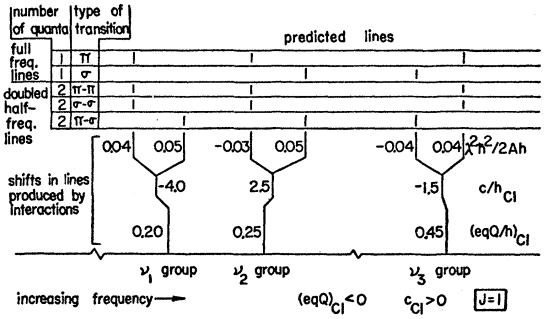

FIG. 5. Predicted weak-field spectrum.

[22] L. I. Schiff, *Quantum Mechanics* (McGraw-Hill Book Company, Inc., New York, 1949), first edition, pp. 207–208.

[23] D. Bohm, *Quantum Theory* (Prentice-Hall Inc., New York, 1951), first edition, pp. 498–499.

[24] See reference 22, p. 190.

Hughes and Grabner[6] for the Stark effects due to a weak static field. With

$$H(t)=\frac{\hbar^2}{2A}\mathbf{J}^2+H_Q-\boldsymbol{\mu}\cdot(\mathbf{E}_{\rm dc}+\mathbf{E}_{\rm rf}\cos\omega t), \quad (8)$$

solutions to (3) are obtained with time-independent perturbation theory. $E_{\rm dc}$ and $E_{\rm rf}$ are assumed to be small enough that the weak field representation and approximations may be used. The second-order "energy" is

$$E(J,I,F,m_F,t)=E(J)+E_Q(F)+d(F,m_F)(E_{\rm dc}+E_{\rm rf}\cos\omega t)^2, \quad (9)$$

and the first-order wave functions are[25]

$$u(J,I,F,m_F,t)=\sum_{m_I,m_J}c(F,m_F;m_I,m_J)\times\Phi(J,m_J)\Phi(I,m_I)+g(E_{\rm dc})\Phi(J\pm1,m_J)+k(E_{\rm rf})\Phi(J\pm1,m_J)\cos\omega t, \quad (10)$$

where $g(E_{\rm dc})$ and $k(E_{\rm rf})\ll1$. The transition probabilities to be discussed do not involve changes in J, so for simplicity $E(J)$ will be dropped from expressions for energy differences. As the third member in (9) is smaller than the second by a factor of the order of 10^2 or more, the approximation

$$E(J',I,F',m_{F'},t)-E(J,I,F,m_F,t)\cong E_Q(F')-E_Q(F) \quad (11)$$

can be used in the denominator of (7). The orders of magnitude of $\langle J',I,F',m_{F'}|\partial H'(t)/\partial t|J,I,F,m_F\rangle$ will now be examined. The π component of the radio-frequency field leads to matrix elements which signify changes in F without changes in m_F, and only such elements will be considered as all the observed transitions were of this type. Two types of time dependence are found. If the first and second members of (10) are considered in the initial and final states terms with $\sin\omega t$ time dependence are produced (type 1), while when the first and third members are used in the initial and final states, respectively, terms with $\sin\omega t\cos\omega t$ time dependence arise (type 2). The exponential term in (7) becomes

$$\exp\left\{\frac{-i}{\hbar}\left[(E_Q(F')-E_Q(F))t+(d(F',m_{F'})-d(F,m_F))\times\left[E_{\rm dc}^2+\frac{2E_{\rm dc}E_{\rm rf}\sin\omega t}{\omega}+E_{\rm rf}^2\left(\frac{t}{2}+\frac{\sin2\omega t}{4\omega}\right)\right]\right]\Big|_{t_0}^{t}\right\}. \quad (12)$$

All the $\sin\omega t$ terms in (12) are expanded with the aid of the relation[26]

$$\exp[ix\sin nt]=\sum_{-\infty}^{\infty}J_n(x)\exp[int]. \quad (13)$$

The expression for (12) then contains two infinite series of Bessel functions with arguments $[E_{\rm dc}E_{\rm rf}\{d(F',m_{F'})-d(F,m_F)\}]/\omega$ and $[E_{\rm rf}^2\{d(F',m_{F'})-d(F,m_F)\}]/4\omega$. These arguments are always of the order of 10^{-2} or less in the present experiments, so each series may be replaced by one. The simplified form of the exponential (12), the approximate denominator (11), and the two types of time dependence of $\langle|\partial H'(t)/\partial t|\rangle$ are now used to form $a(J,I,F',m_{F'})^{(1)}$, as given by integration of (7). The frequencies for which the denominator of the expansion coefficient vanish are interpreted as resonance frequencies. Since these denominators are real and the numerators are nonvanishing, these resonance frequencies are the same as the resonances in $|a(J,I,F',m_{F'})^{(1)}|^2$ which is proportional to the transition probability[27] from the F,m_F to the $F',m_{F'}$ state. If the type 1 time dependence is used, the denominator of the integral of (7) vanishes when

$$\omega=\pm\frac{1}{\hbar}\left[E_Q(F')-E_Q(F)+\{d(F',m_{F'})-d(F,m_F)\}\left(E_{\rm dc}^2+\frac{E_{\rm rf}^2}{2}\right)\right]. \quad (14)$$

Except for the contribution of the radio-frequency field, this is the same as the result of Hughes and Grabner.[6] The frequency shift due to $E_{\rm rf}$ is

$$\Delta\nu=\left\{\frac{d(F',m_{F'})-d(F,m_F)}{h}\right\}\frac{E_{\rm rf}^2}{2}. \quad (15)$$

If the type 2 time dependence is used, the resonant denominator vanishes when

$$\omega=\pm\tfrac{1}{2}\hbar[E_Q(F')-E_Q(F)+\{d(F',m_{F'})-d(F,m_F)\}(E_{\rm dc}^2+\tfrac{1}{2}E_{\rm rf}^2)]. \quad (16)$$

These resonances are at exactly one half of the frequency of those given by (14). The frequency shift in the doubled half-frequency is also given by (15). Except for this radio-frequency shift, "half-frequency" resonances were predicted by Hughes and Grabner,[6] and were studied extensively in the present experiment. Also in agreement with Hughes and Grabner, it can be seen from (10) that since the type 1 time dependence of $\langle|\partial H'(t)/\partial t|\rangle$ vanishes, the full frequency transitions are forbidden when $E_{\rm dc}=0$.

In the second case of interest to the LiCl electric resonance experiments the perturbation due to $E_{\rm dc}$ is considered much larger than E_Q which is neglected.

[25] The coefficients $c(F,m_F;m_I,m_J)$ are discussed in E. U. Condon and G. H. Shortley, *Theory of Atomic Spectra* (Cambridge University Press, Cambridge, 1951), first edition, pp. 73–78.

[26] H. Jeffries and B. S. Jeffries, *Methods of Mathematical Physics* (Cambridge University Press, Cambridge, 1950), second edition, p. 589.

[27] Reference 22, p. 192.

Both the π and σ components of the radio-frequency field are important and are included separately. The strong field representation is used and (3) is solved[28] to find $u(J,m_J,t)$ with first-order time-independent perturbation theory, while $E(J,m_J,t)$ is found with second-order theory. It is first assumed that E_{dc} is much greater than E_{rf}. In this case, a good approximation for the denominator of (7) is

$$E(J',m_{J'},t)-E(J,m_J,t)\simeq\{b(J,m_{J'})-b(J,m_J)\}E_{dc}^2. \quad (17)$$

The $\sin\omega t$ terms in the exponential in (7) are again expanded with (13). The arguments of all the Bessel functions are all much less than one so that each series is equal to one. The largest term in $\langle|\partial H'(t)/\partial t|\rangle$ connects states with $m_{J'}=m_J\pm1$ and has type 1 time dependence. When the simplified exponential is used with (17) and the type 1 time dependence to form (7) and the integration is performed the denominator of the result is found to be zero when

$$\omega=\pm\frac{1}{\hbar}\{b(J,m_J\pm1)-b(J,m_J)\}\times\left(E_{dc}^2+\frac{(E_{rf\pi}^2+E_{rf\sigma}^2)}{2}\right). \quad (18)$$

Except for the frequency shift due to E_{rf},

$$\Delta\nu=\left\{\frac{b(J,m_J\pm1)-b(J,m_J)}{h}\right\}\left(\frac{E_{rf\pi}^2+E_{rf\sigma}^2}{2}\right), \quad (19)$$

this transition frequency is the same as that predicted by the strong-field theory of Hughes and Grabner.

If E_{rf} is considered small enough that (18) is still a fairly good approximation for the denominator of (7), but somewhat larger than in the previous case, terms in $\langle|\partial H'(t)/\partial t|\rangle$ with type 2 time dependence and with $m_{J'}=m_J\pm1$ or $m_J\pm2$ must be included. The arguments of the Bessel functions obtained when the exponential in (7) is expanded are still considered small enough that each series may be replaced by one. Combining (18), the simplified exponential, and the type 2 time dependence, the denominator obtained when (7) is integrated vanishes when

$$\omega=\pm\frac{1}{2}\frac{1}{\hbar}\{b(J,m_J\pm1)-b(J,m_J)\}\times\left[E_{dc}^2+\frac{(E_{rf\pi}^2+E_{rf\sigma}^2)}{2}\right]. \quad (20)$$

These resonances are at exactly one half the frequency given by (18) and the frequency shift in the doubled half-frequency is given by (19). Except for the radio-frequency shift, such resonances were first predicted and observed by Hughes and Grabner.

[28] Matrix elements needed to form $E(J,m_J,t)$ and $u(J,m_J,t)$ are given in reference 1.

Similar methods may be used to obtain the results given by Townes and Merritt.[4] The molecule is assumed to be a rotating dipole which moves in high- and low-frequency fields with strengths E_H and E_L and angular frequencies ω_H and ω_L, respectively. E_H and E_L are assumed to be in the same direction. Rotational transitions are produced by E_H. The quantity ω_H is of the order of 10^4 Mc/sec while ω_L is of the order of 1 Mc/sec or less. (3) is solved with the strong-field theory, and a good approximation for the denominator of (7) is

$$E(J',m_J',t)-E(J,m_J,t)\cong E(J+1)-E(J), \quad (21)$$

if terms smaller than this by the order of 10^3 are neglected. $\langle J+1,m_J|\partial H'(t)/\partial t|J,m_J\rangle$ is proportional to $\mu\omega_H E_H\sin\omega_H t$ when terms smaller by 10^4 are neglected.

Two cases are discussed by Townes and Merritt. In the first case, ω_L is considered so small that the time available for absorption or radiation in the gas, $(t-t_0)$, is much less than $1/\omega_L$, and the approximations

$$\sin[\omega_L(t-t_0)]\simeq\omega_L(t-t_0) \quad (22)$$

and

$$\cos[\omega_L(t-t_0)]\simeq\cos2\omega_L t_0, \quad (23)$$

may be used to simplify the exponential in (7). The $\sin\omega_H t$ terms are expanded by means of (13), and the arguments of all the Bessel functions are of the order of 10^{-5} or less so that each series is equal to one. When (7) is formed and integrated with these approximations, the denominator vanishes when

$$\omega_H=\pm\frac{1}{\hbar}\left\{E(J+1)-E(J)-[b(J+1,m_J)-b(J,m_J)]\times\left(\frac{E_H^2}{2}+E_L^2\cos^2(\omega_L t_0)\right)\right\}. \quad (24)$$

If E_H is so weak that it does not observably change the resonance frequencies, the frequency shift due to E_L is

$$\Delta\nu=\left\{\frac{b(J+1,m_J)-b(J,m_J)}{h}\right\}E_L^2\cos^2(\omega_L t_0), \quad (25)$$

the result given by Townes and Merritt.

In the second case, $(t-t_0)$ is greater than or about equal to $1/\omega_L$ and (23) is a poor approximation. Both the $\sin\omega_L t$ and $\sin\omega_H t$ terms in the exponential in (7) are expanded with (13). In addition to Bessel functions with very small arguments, a series with the argument $\{b(J+1,m_J)-b(J,m_J)\}E_L^2/4\hbar\omega_L$ is found. As this argument may be of the order of one or larger, this series must be retained. When (7) is formed with these approximations and integrated, the denominator

vanishes when

$$\omega_H=\pm\frac{1}{\hbar}\left\{E(J+1)-E(J)+[b(J+1,m_J)-b(J,m_J)]\times\left(\frac{E_H^2}{2}+\frac{E_L^2}{2}\right)\right\}+2n\omega_L. \quad (26)$$

If, as before, shifts due to E_H are unobservably small, the frequency shift due to E_L is

$$\Delta\nu=\left\{\frac{b(J+1,m_J)-b(J,m_J)}{h}\right\}\frac{E_L^2}{2}+2n\nu_L, \quad (27)$$

the result given by Townes and Merritt.

The relative intensities of resonances corresponding to different n values are expected to be proportional to the ratios of $|a(J+1, m_J)|^2$ for different n values. Thus if the fields are held fixed, the relative intensities will be proportional to the ratios of $J_n^2\{b(J+1, m_J)-b(J,m_J)\}E_L^2/4\hbar\omega_L$ for different n values, a result stated by Townes and Merritt.

The main difference between the general method used above and the earlier calculations of the resonance frequencies is that in the earlier theory, approximate solutions to (1) and expansion coefficients analogous to (4) are based on solutions to the time-independent Schrödinger equation instead of (3). The interpretation of (4) in terms of the transition probability is believed to be justified because (3) and the time-independent Schrödinger equation describe the molecular motion equally well before the molecules enter the C-field, and because in both theories (1) is taken as the only true equation while the molecules are in the C-field.

Autler and Townes[29] have recently and independently developed a theory for the radio-frequency field effects by much more general methods. The present results may be derived from this general theory; however, they have not obtained the results of specific interest to the present experiments.

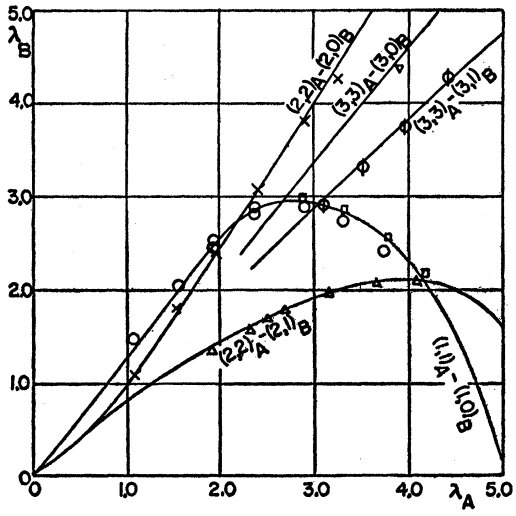

FIG. 6. λ_A required to refocus several different states, as a function of λ_B. Curves are predicted refocusing conditions. Points are observed refocusing conditions.

[29] S. H. Autler and C. H. Townes, Phys. Rev. **100**, 703 (1955).

RADIO-FREQUENCY STARK EFFECT IN PREVIOUS ELECTRIC RESONANCE EXPERIMENTS

It is necessary to show that the theory developed for the radio-frequency Stark effect is consistent with the absence of such effects in previous experiments. In all these experiments except those of Braunstein and Trischka,[9] the σ connection of the C-field electrodes was used. It is impossible to calculate the radio-frequency field in these cases because the position of the beam in the C-field is not given.

However, in Braunstein and Trischka's experiment the beam position was the same as in the present work, so that the radio-frequency field could be calculated from the voltage with the results given in Fig. 4. The radio-frequency Stark effect was estimated for all their observations.[30] Refined calculations were impossible because the variation of the line strengths with radio-frequency field were not studied in the strong field observations with the π connection, and the intensities of the individual weak field lines cannot be reliably determined. However, when the most reasonable guesses were made, the predicted radio-frequency Stark effects were all less than or about equal to the experimental errors. Thus the absence of observed radio-frequency Stark effect in these experiments is not inconsistent with the theory.

IDENTIFICATION OF STATES

Complete consistency with all the predicted lines was the best proof that the observed lines were correctly identified. However, in the earlier stages of the study it was helpful to identify the initial and final strong field states of individual lines by a study of the line intensities as a function of the deflecting field strengths. This was done by a new method which will now be described.

The relations between the field parameter, $\lambda=2\mu AE/\hbar^2$, and the force on a molecule in an inhomogeneous field have been given by Luce and Trischka[7] for different (J,m_J) states. From these results and the geometry of the apparatus, it was possible to calculate the pairs of λ values that would cause molecules in given (J,m_J) states in each field to be deflected to the detector wire. These pairs are plotted to give the curves shown in Fig. 6. Each curve is the locus of λ_A and λ_B values at which a line with the initial and final (J,m_J) states for the curve should be observable.

When a line was identified with the help of these curves, the oscillating and static components of the

[30] This includes the unpublished weak field observations in R. Braunstein, Ph.D. thesis, Department of Physics, Syracuse University, Syracuse, New York, January, 1954 (unpublished).

C-field were held fixed. With the B-field held fixed, the A-field was varied and the line intensity was observed to pass through a maximum. The line intensity was remeasured at different B-field strengths. When the correct value of μA was selected, the field strengths which gave maximum intensity coincided with one of the calculated curves. The quantity μA was found to be 3.0×10^{-56} cgs units by this method. The probable error due to imperfect calibration of the fields and errors in the apparatus alignment is $\pm30\%$.

Lines produced with $(2,2)_A$–$(2,0)_B$, $(2,2)_A$–$(2,1)_B$ and $(3,3)_A$–$(3,0)_B$ as the states in the A- and B-fields, respectively[31] were also studied to test the method and are included in Fig. 6. The identification of these lines was confirmed by the agreement between the observed and predicted frequencies.

When spectra for the determination of the interaction constants were studied, the A- and B-fields were adjusted to 6500 and 6800 v, respectively. These gave $\lambda_A=2.9$ and $\lambda_B=3.0$, and gave the best signal-to-noise ratio in the spectra because the force in the B-field was maximized.

OBSERVED SPECTRA

Spectra were observed at zero static field and at (weak) field strengths of 7.660 and 15.32 v/cm. In these observations, the static field was held fixed and the detector current change produced when the radio-frequency field was turned on or off was measured at frequencies spaced one-half kc/sec apart for the half-frequency lines and one kc/sec apart for the full-frequency lines. The individual lines were well resolved in almost all cases. The half-width of the full-frequency lines was about $9\frac{1}{2}$ kc/sec, about double the width of the half-frequency lines. As the line broadening due to the C-field inhomogeneity was negligible, the theoretical half-width[5] was $1.07/\tau$, where τ is the time of flight through the C-field for molecules with the most probable velocity. For an oven temperature of 805°K and an effective field length of 8 cm, the calculated half-width was 7.6 kc/sec, about 1.9 kc/sec less than the observed half-width.

Three lines, one from each group shown in Fig. 5, were observed for each isotopic species and vibrational state. In the following discussions, it is convenient to classify the lines by the Cl isotopic species and vibrational state of the molecules which underwent a transition. Thus the three strongest lines, assigned to Li^6Cl^{35} in the zeroth vibrational state, will be referred to as 35–0 lines. At zero static field only half-frequency lines could be observed and the 35–0 lines were studied extensively. At 7.660 v/cm, the full-frequency lines of all isotopic species were studied, and at 15.32 v/cm both full- and half-frequency 35–0 lines were studied.

The 35–0 lines were observed with several different radio-frequency field strengths and both C-field connections shown in Fig. 2, at zero field and with both weak fields. Radio-frequency voltages were measured with a meter similar to the Hewlett-Packard model 410-A calibrated in the laboratory by comparison with three other radio-frequency voltmeters.

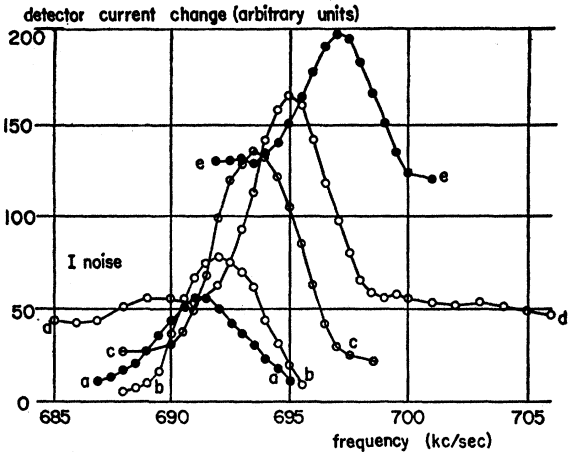

FIG. 7. Frequency-insensitive background and radio-frequency Stark effect in the highest frequency 35–0 line observed as a half-frequency line at zero static field. Curve a: $V_{rf}=7.05$ v, b: $V_{rf}=8.8$ v, c: $V_{rf}=11.2$ v, d: $V_{rf}=13.9$ v, e: $V_{rf}=15.5$ v. π connection of the C-field electrodes.

The static field strengths were calculated from the electrode separation, 0.65268 cm, and the applied voltage. The voltage was measured with a Leeds and Northrup model K-1 potentiometer used with an Eppley Standard Cell calibrated by the National Bureau of Standards, and a Leeds and Northrup voltbox. Frequency measurements were made with a General Radio Company model 616-D frequency meter calibrated against commercial broadcasting stations.

Figure 7 shows several observations made at zero static field on the line which will later be identified as the highest frequency half-frequency 35–0 line. At large radio-frequency fields, the line appears to rise above a frequency-insensitive background. Other observations showed that the background extended at least 200 kc/sec above or below the line center frequency and, except for other sharp lines, had uniform intensity. Such backgrounds were never observed in strong-intermediate field measurements.

One possible explanation of this background is found in the variation of the residual beam with C-field strength. The residual beam was much smaller than the refocused beam when the static field was 220 v/cm or larger, but increased slowly and then more rapidly as the field was decreased, until at zero field it was about equal to the refocused beam. Because of this nonlinearity, the average beam should increase when the radio-frequency field was turned on. Estimates of the detector current change produced by this process showed that it was the same as the observed background

[31] The $(3,3)_A$–$(3,0)_B$ line was observed as a full-frequency line, (single-quantum transition), with a weak static C-field.

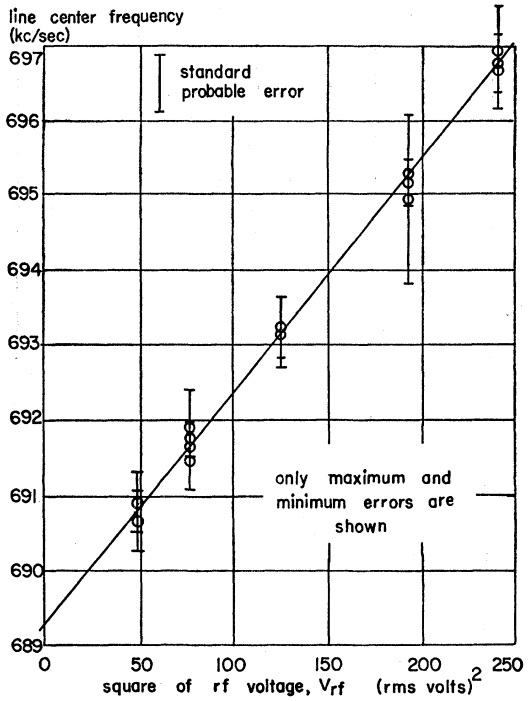

FIG. 8. Linear relationship between the observed line-center frequency and the square of the radio-frequency voltage, (radio-frequency Stark effect), for the highest frequency 35–0 line as observed at zero static field as a half-frequency line, with the π connection of the C-field electrodes.

within the large errors in the observations of the C-field —residual beam relationship.

Because of the reduced beam, the noise in the detector current was smaller for the large-field measurements than for those at zero or weak fields and hence the weakest lines, produced by molecules in higher vibrational states, could only be observed with large fields. Measurements with a large field were also necessary to determine $\mu^2 A$.

Preliminary observations, with the static field such that the strong-field approximation could be used for the analysis, gave lines more than four times as broad as the weak field lines. This broadening, caused by the C-field inhomogeneity, would have reduced the accuracy of $(eqQ)_{Cl}$ or c_{Cl} values calculated from these data, and, as a compromise, observations were made at a strong-intermediate field strength of about 384 v/cm, which gave lines with about 10.3 kc/sec half-width.

At 384 v/cm, a group of six lines of approximately equal intensity was found for each isotopic species and vibrational state, in agreement with the prediction obtained with the strong field selection rules. For these measurements the oscillator frequency was held fixed, while the static field strength was varied in small steps so that eight to ten points were observed between the half-maxima of each line. The oscillator was kept in continuous zero beat with a harmonic from the calibration crystal oscillator in a General Radio Company, model 620-A frequency meter. The crystal frequency was frequently checked against radio station WWV. All the measurements were made with the static field adjusted to cause the lines to fall as nearly at 384 v/cm as permitted by the spacing of the calibration oscillator harmonics.

It was also desirable to make measurements with a smaller field because the frequency of the seventh line, predicted by the intermediate-field theory, could be used to determine the sign of $(eqQ)_{Cl}$ directly. When the 35–0 lines were studied with a static field of 231 v/cm, the seventh line was found with intensity 45% as great as the other six.

ANALYSIS OF THE SPECTRA

As the first step in the identification of the isotopic species and vibrational states of the zero- and weak-field lines, the three most intense lines were assigned to Li^6Cl^{35} in the zeroth vibrational state. Similar groups of three lines of lower intensity were assigned to the higher vibrational states of Li^6Cl^{35} and to Li^6Cl^{37} in different vibrational states. This assignment could be made entirely from the assumption that the population of vibrational states followed the Boltzmann distribution, and to satisfy the known ratio of $(eqQ)_{Cl^{35}}$ to $(eqQ)_{Cl^{37}}$.[32] The presence of three lines for each isotopic species indicated that $(eqQ)_{Cl}$ was negative.

Figure 5 shows that if both π and σ transitions occurred simultaneously, as might be expected with the σ connection of the electrodes, groups of two closely spaced lines should have appeared in the weak field spectra of each isotopic species and vibrational state. With an approximate value of $\mu^2 A$ obtained from the analysis of the strong-intermediate field data with the strong-field approximation, it was shown that the individual lines in these groups should have been well resolved in the observations at 15.32 v/cm. However, the magnitude and sign of the observed Stark effect, as well as the absence of groups of two lines, showed that the observed lines were π transitions, and that no σ transitions occurred. Their absence is explained by the relative weakness of the σ component obtained with the σ connection; Fig. 4 shows that the π component was two to six times as large as the σ component.

Figure 7 shows the frequency shift caused when different radio-frequency fields were used to produce the highest frequency 35–0 line at zero static field as a half-frequency line. In Fig. 8, the center frequencies of these lines are plotted against the square of the radio-frequency voltage, V_{rf}. All the observed line center frequencies fall on a straight line on this graph. Similar relations were found for all the other zero and weak field lines. Thus, in qualitative agreement with (15),

[32] Wang, Townes, Schawlow, and Holden, Phys. Rev. 86, 809 (1952).

the radio-frequency field dependence of the line center frequencies, ν, could be represented by

$$\nu=\nu_0+\eta V_{rf}^2, \tag{26}$$

where ν_0 is the line center frequency in the absence of a radio-frequency field, and η is a constant which is different for each line. The constants ν_0 and η, given in Table I, were calculated by a weighted least-squares method[33] for all the Li^6Cl^{35} lines observed at zero or weak static fields with both C-field connections and different radio-frequency fields. The systematic procedure used to estimate the weights took account of the change in the refocused beam during the observation of a line, the size of the background of transitions if present, the signal-to-noise ratio, and the resolution of the line. The errors in ν_0 and η were determined from the errors in the line center frequencies.[34] The probable errors in lines of unit weight were estimated by comparison of repeated measurements of a line and from the errors in the frequency measurements to be ± 0.7 kc/sec for the full-frequency lines and ± 0.4 kc/sec for the half-frequency lines.

All of the observed shifts might be accounted for if part of the radio-frequency voltage was rectified at some point in the C-field wiring and appeared as an "extra" static field. To test this hypothesis, the highest frequency 35–0 line was studied with a 7.660-v/cm static field applied with the polarity reversed. With reversed polarity any rectified voltage would reduce rather than increase the static field and modify the frequency shift due to the radio-frequency field. The ν_0 and η values found from these observations are inincluded in Table I. They agree well with those obtained with the "direct" connection, which shows that any rectified voltage was too small to be observed. This result was confirmed by observation of the voltage on the C-field electrodes with an oscillograph, and the upper limit of the rectified voltage was estimated to be $\pm 5\%$ of V_{rf}.

Equation (15) was used to calculate the theoretical values of η given in Table I. The intermediate-field theory was used to calculate the Stark effect, as the weak-field approximation was found to be inaccurate for the largest radio-frequency fields used in the observations. The ratio V_{rf}/E_{rf} was needed for these calculations, but with the σ connection it could not be estimated very reliably because of the variation of the field over the beam height. In these cases an "effective" ratio was estimated from observations of the variation of the line intensities with radio-frequency field made with the π connection, and the field distribution shown in Fig. 4.

Table I shows that the theoretical and experimental values of η agree within the experimental error, except for the highest frequency 35–0 line observed at zero static field. Agreement is secured in this case as well if the radio-frequency voltmeter calibration error, $\pm 3\%$, is included in the observed η value. Because of the uncertainty in the calculated values, the agreement between the calculated and observed η values with the σ connection is much less significant than with the π connection.

TABLE I. Line-center frequencies at zero radio-frequency field and radio-frequency Stark effect coefficients calculated from observations of the three 35–0 lines with zero and weak static fields.[a]

Field connection	ν_0 (kc/sec)	η (obs) (kc/sec-v^2) $\times 10^2$	η (calc) (kc/sec-v^2) $\times 10^2$
	$E_{static}=0.0$ v/cm[b]		
π	606.08±1.31	−5.03±1.68	−5.04
π	773.28±0.92	−2.79±2.2	−3.78
π	1378.52±0.52	6.18±0.35	5.52
	$E_{static}=7.660$ v/cm		
σ	604.60±0.71	−1.4 ±1.1	−2.1
σ	772.72±0.89	0.4 ±1.9	−1.5
σ	1380.37±0.46	2.00±0.42	2.18
σ[c]	1380.42±0.75	2.38±0.63	2.18
π	1380.89±0.71	5.58±0.54	5.45
	$E_{static}=15.32$ v/cm		
σ	601.21±0.37	0.8 ±1.2	<2
σ	769.3 ±1.0	···	
σ	1384.52±0.42	1.18±0.37	<2

[a] ν_0 is the line-center frequency in the absence of radio-frequency field calculated from the observations with (26). η is the radio-frequency Stark effect coefficient calculated from the observations with (26) and from the theory with (15).
[b] The observed values of ν_0, and observed and calculated values of η, have been multiplied by two for these half-frequency observations.
[c] Polarity of static field reversed.

The radio-frequency Stark effect was studied experimentally only in the 35–0 lines. Because of the uncertainties in a direct calculation of the radio-frequency field from the applied voltage with the σ connection, lines in higher vibrational states were corrected for this effect with η values determined from the 35–0 data as modified to take into account the changes in μ^2A with vibrational state and isotopic species. The μ^2A values were obtained from an approximate analysis of the strong-intermediate field data with the strong-field theory.

After correction for the radio-frequency Stark effect, the Stark effects caused by the static field were calculated from the μ^2A values and static field strengths with the weak field theory, and subtracted from the observed frequencies to obtain the line frequencies in the absence of all fields. The field-corrected frequencies of all the zero- and weak-field lines are given in Table II. $(eqQ)_{Cl}$ and c_{Cl} values were calculated from these frequencies by a least-squares method to secure the best agreement between the three lines for each isotopic species and vibrational state, and the two constants. In this calculation, each line frequency was weighted according to its probable error, with the

[33] A. G. Worthing and J. Geffner, *Treatment of Experimental Data* (John Wiley and Sons, Inc., New York, 1943), p. 243, Eqs. (21), (22), and (23).
[34] R. H. Bacon, Am. J. Phys. **21**, 428 (1953), especially Eqs. (59) and (61).

TABLE II. Observed and calculated line-center frequencies of the zero- and weak-field lines, corrected for radio-frequency and static-field Stark effects.

Cl isotope and vib state	Line-center frequencies (kc/sec) Observed	Calculated[a]
	Static field = 0.0 v/cm	
35–0	606.08±1.31[b]	606.08
35–0	773.28±0.92[b]	773.12
35–0	1378.52±0.52[b]	1379.21
	Static field = 7.660 v/cm	
35–0	605.86±0.71	same as
35–0	773.66±0.89	above
35–0	1379.11±0.46	
35–0	1379.16±0.75[c]	
35–0	1379.63±0.71[b]	
35–1; 37–1	687.06±0.83	687.13
35–1	875.4 ±1.1	875.53
35–1	1562.72±0.82	1562.66
37–0	476.49±0.89	476.48
37–0	1086.2 ±1.0	1086.19
	unresolved	607.7
35–2	765.2 ±1.2	765.8
35–2	973.7 ±1.2	973.7
35–2	973.0 ±1.2	973.7
35–2	1739.9 ±1.1	1739.5
37–1	540.31±0.85	540.6
37–1	540.79±0.90	540.6
35–1; 37–1	686.4 ±3.6	687.7
37–1	1228.9 ±2.9	1228.3
	Static field = 15.32 v/cm	
35–0	606.25±0.37	as above
35–0	773.08±1.0	for
35–0	1379.48±0.42	35–0

[a] Line-center frequencies calculated with interaction constants determined from zero- and weak-field observations.
[b] π connection of the C-field electrodes. All other data were obtained with the σ connection.
[c] Reversed static field polarity.

errors in the corrections for radio-frequency Stark effect included. The errors in the interaction constants were calculated by the methods and equations in reference 34.

The assignment of isotopic species and vibrational states to the lines in the strong-intermediate field spectrum is given in Table III. The methods used to identify the isotopic species and vibrational states of the lines were the same as for the weak-field spectra.

Past observations with the present apparatus have shown that when a given line is observed repeatedly with a fixed oscillator frequency, slightly different C-field voltages are required for the line center. The cause of this C-field "drift" has not been found. The maximum variation in field in all the present observations was 5 parts in 10^4, although in a period of two to three hours the variation was always less than 2 parts in 10^4. To reduce the error in the determination of frequency differences, the lowest frequency 35–0 line was selected as a reference line, and measurements of all the other lines were preceded and followed by observations of this reference line. A series of observations of the reference line made after voltage had been applied to the C-field electrodes and voltbox for eight hours or more were judged to be the most reliable and the average field for these observations disagreed by less than 1 part in 10^5 with the average for all the reference line measurements. For the analysis, the average field for the most reliable measurements was selected as a standard field and the differences between the standard field and the fields observed for the reference lines were used to correct all the lines for C-field drift.

Several observations of the reference line were made with the polarity of the C-field reversed. The reasons for a difference in the field required to produce a line with reversed and direct polarity have been discussed before.[8,9] The average observed difference in field was 0.056 v/cm, and half of this difference was added to the field strength of each direct-polarity observation to correct for the residual potentials in the wiring and C-field electrodes.

Values of $(eqQ)_{Cl}$ and μ^2A were calculated from the corrected observations by a method of successive approximations that used both the strong- and the intermediate-field theories. As the first step, the frequency that each observed line would have at the standard field was calculated with the strong-field theory and an approximate μ^2A. Comparison with the intermediate-field theory showed that the final error introduced by use of the strong-field theory for this adjustment was less than one-quarter of the experimental error in all cases. Next, line frequencies were predicted for the standard field with the intermediate-field theory, with approximate $(eqQ)_{Cl}$ and μ^2A values, and with the c_{Cl} value obtained from the weak field spectra. These frequencies were compared with the adjusted corrected observed frequencies. Guided by the strong field theory, new $(eqQ)_{Cl}$ and μ^2A values were selected, the adjustments to the standard field were remade, and the readjusted corrected observed frequencies were compared with the frequencies predicted by the intermediate field theory with the improved constants. When this procedure had been repeated until the observed and predicted frequencies agreed to within eight kc/sec or less, the strong-field theory was used to correct the last approximation and obtain the final constants. As a check on this last step, the final constants for Li^6Cl^{35} in the zeroth vibrational state were resubstituted into the intermediate-field theory and the predicted frequencies were found to agree with the adjusted corrected observed 35–0 line frequencies within the experimental error. The adjusted corrected frequencies of all the strong-intermediate field lines are given in Table III.

No attempt was made to calculate c_{Cl} values from the strong-intermediate field data. The c_{Cl} values determined from the weak-field data were inserted in the equations at the start of the calculations and were not changed.

Slight modifications in the procedure outlined above were needed in the analysis of the 35–3 and 37–2 ob-

servations. A c_{Cl} value for Li^6Cl^{35} in the third vibrational state was not available from the weak-field observations because the lines were too weak. Since no systematic variation in this constant was observed in the first two vibrational states, the value for Li^6Cl^{35} in the zeroth state was used in the analysis. Since only one 37–2 line was observed, it was necessary to assume values for both $(eqQ)_{Cl}$ and c_{Cl} to calculate μ^2A from this line. The ratio $(eqQ)_{Cl^{35}}/(eqQ)_{Cl^{37}}$ is approximately equal to the ratio of the change in $(eqQ)_{Cl^{35}}$ from the zeroth to the first vibrational state to the corresponding change in $(eqQ)_{Cl^{37}}$, and it is expected that a similar relation would hold between the first and second vibrational states. The weak-field interaction constants for Li^6Cl^{37} in the first vibrational state were used with this assumption to give $(eqQ)_{Cl^{37}}=-3046.6$ kc/sec in the second vibrational state. The error in this value, ±8.8 kc/sec, is taken as the sum of the errors in $(eqQ)_{Cl^{37}}$ in the first vibrational state and the change in $(eqQ)_{Cl^{37}}$ from the first to the second state. The calculated $(eqQ)_{Cl^{37}}$ value and the weak-field c_{Cl} value for Li^6Cl^{37} in the zeroth vibrational state were used with the methods described above to obtain μ^2A.

TABLE III. Observed and calculated line-center frequencies of the strong-intermediate field lines. The observed values have been corrected and adjusted.[a]

Cl isotope, vib state, and line number[b]	Line-center frequencies (kc/sec) Observed	Calculated[c]
35–0–1	11 003.0[d]	11 003.0
35–0–2	11 390.1	11 390.2
35–0–3	11 617.4	11 616.4
35–0–3	11 616.5	11 616.4
35–0–4	12 106.2	12 106.3
35–0–5	12 325.2	12 324.9
35–0–6	12 719.9	12 719.5
35–0–6	12 719.3	12 719.5
35–1–1	11 335.0	automatic
35–1–6	13 279.5	agreement
35–2–1	11 688.5	automatic
35–2–6	13 854.7	agreement
35–3–1	12 065.5	12 064.8
35–3–1	12 064.2	12 064.8
35–3–3	12 912.0	12 913.0
35–3–3	12 911.7	12 913.0
35–3–6	14 438.8	14 439.4
35–3–6	14 440.0	14 439.4
35–3–6	14 446.6	14 439.4
37–0–1	11 270.1	11 270.8
37–0–1	11 271.2	11 270.8
37–0–5	12 311.8	12 311.6
37–0–6	12 624.2	12 624.3
37–1–1	11 630.1	11 630.3
37–1–2	11 974.6	11 974.6
37–1–4	12 613.4	12 612.2
37–1–6	13 159.9	13 159.3
37–2–6	13 710.4	automatic
	13 710.2	agreement

[a] The observed values have been corrected for C-field drift and residual emf's, and have been adjusted to the standard field, 383.65 v/cm.
[b] Numbering of lines as given in reference 6 for (1, 1–1, 0) spectrum at strong fields.
[c] Calculated with interaction constants determined from strong-intermediate field observations.
[d] Reference line.

TABLE IV. Probable errors in the observed strong-intermediate field lines given in Table III.

Source of error	Probable error (kc/sec)
(a) Probable random errors	
Wavemeter and oscillator frequency calibration	±0.3
Reference line error due to C-field drift	±0.5
Uncertainty in reference line due to noise and limited number of data points	±0.9
C-field static voltage setting	±0.15
Uncertainties in line centers due to noise and limited number of data points; isotopic species and vibrational states of lines given below:	
35–0	±0.9
35–1; 37–0	±1.5
35–2; 37–1	±2.7
35–3; 37–2	±6.0
(b) Probable systematic errors	
Voltbox calibration (2 parts in 10^4 in voltage)	±4.7
Standard cell calibration (1 part in 10^4 in voltage)	±2.3
Potentiometer calibration (1 part in 10^4 in voltage)	±2.3
C-field drift; uncertainty in true line center field strength	±10.0

So far, the second-order perturbation theory results have been used to analyze the Stark effect. The additional term introduced by the fourth order theory[1] is proportional to $\mu^4A^3(E_{static})^4$, and may be found experimentally from the deviation of the Stark effect from quadratic field dependence. With the maximum field strength available in the present apparatus, the deviation was too small to give μ^4A^3 reliably for LiCl, and hence μ and A were not obtained separately from the spectra. A correction of $3.595\times10^{107}\,\mu^4A^3$, where μ and A are in cgs units, should be added to the results obtained with the second order theory and given in Table V. The static field strength was inserted into the fourth order theory to obtain this correction. Estimated values[20] of μ and A show that the correction is about 4 parts in 10^4.

An experimental study showed that in the strong-intermediate field observations the radio-frequency Stark effect, if present, was much smaller than the experimental errors. Calculations made with (19) confirmed this observation.

The random errors in the strong-intermediate field observations are given in Table IV(a) expressed in terms of equivalent frequency errors in the lines. The equivalent error introduced from the error in the weak-field c_{Cl} values was less than ±0.2 kc/sec at most, and hence negligible. For calculation of the random errors in $(eqQ)_{Cl}$ and c_{Cl}, the total errors in the lines were taken as the square root of the sum of the squares of the errors given in Table IV(a), and it was assumed that the most widely separated lines determined the constants entirely. The errors in the interaction constants

TABLE V. Nuclear-molecular interaction constants, μ^2A values, and ratios derived from the constants, for Li^6Cl.

Constant	$v=0$	$v=1$	$v=2$	$v=3$
for Li^6Cl^{35}				
$(eqQ/h)_{Cl}$ (kc/sec)	−3071.72±0.61	−3479.3 ±1.7	−3873.0 ±1.8	−4250.0±11
$(c/h)_{Cl}$ (kc/sec)	2.07±0.10	2.22±0.20	2.19±0.21	···
μ^2A ($\times10^{76}$ cgs)[a]	1774.26±0.28	1840.26±0.40	1909.3 ±0.6	1980.6±0.9
for Li^6Cl^{37}				
$(eqQ/h)_{Cl}$ (kc/sec)	−2419.9 ±2.4	−2736.6 ±5.4	···	···
$(c/h)_{Cl}$ (kc/sec)	1.88±0.30	1.60±0.34	···	···
μ^2A ($\times10^{76}$ cgs)[a]	1788.24±0.40	1854.9 ±0.6	1924.7 ±0.7	···
$(eqQ)_{Cl^{35}}/(eqQ)_{Cl^{37}}$	1.2694 ±0.0013	1.2714±0.0025	···	···
$\mu^2A(Li^6Cl^{37})/\mu^2A(Li^6Cl^{35})$	1.00788±0.00027	1.0081±0.001	···	···

[a] The random errors in μ^2A are given in the table. The systematic error was $\pm1.1\times10^{-76}$ cgs.

were then calculated from the line errors with the strong-field theory. In the case of Li^6Cl^{37} in the second vibrational state, the error introduced from the calculated $(eqQ)_{Cl}$ value was included.

The systematic errors in the strong-intermediate field data are given in Table IV(b). The major error comes from the C-field drift, which is arbitrarily taken to be the maximum variation found in all the observations of the reference line. The strong-field theory was used to calculate the systematic error in μ^2A as $\pm1.1\times10^{-76}$ cgs. This theory shows that no systematic error in $(eqQ)_{Cl}$ is introduced from systematic errors in the lines.

The sign of $(eqQ)_{Cl}$, already shown to be negative by the weak field observations, was confirmed by the intermediate field observations. The final values of $(eqQ)_{Cl}$, c_{Cl} and μ^2A for Li^6Cl^{35} in the zeroth vibrational state used with the intermediate-field theory to calculate the spectrum at 231 v/cm. The calculated lines agreed, within the experimental error, with the seven most intense observed lines.

FINAL RESULTS AND DISCUSSION

The final values of $(eqQ)_{Cl}$, c_{Cl} and μ^2A are given in Table V. The weak and strong-intermediate field determinations of $(eqQ)_{Cl}$ agreed within the experimental error in all cases. The final values are means of the two determinations weighted by the reciprocals of their errors.[35] The final values of c_{Cl} and μ^2A are the values obtained from the zero- and weak-field data, and from the strong-intermediate field data, respectively.

The sign of $(eqQ)_{Cl}$ in Li^6Cl is the same as in KCl and TlCl, but is opposite to that found in RbCl.[36–38] Townes and Dailey[39] have shown that if the chlorine is covalently bonded, $(eqQ)_{Cl}$ should be −110 Mc/sec, and conclude from the small observed values that alkali-chlorine bonds are primarily ionic. With the assumption that the bond is completely ionic, Inglis[40] has developed a model to predict the sign of (eqQ) in alkali-halides. This model predicts that $(eqQ)_{Cl}$ should have a negative sign in all the alkali chlorides, and the present observations agree with this prediction. A theoretical value of the internuclear distance[20] and the Cl quadrupole moment were used with the Inglis model to calculate $(eqQ)_{Cl}$ in LiCl. The calculated value, −350 kc/sec, is about one ninth as large as the observed values, which suggests that this model is oversimplified.

The observed $(eqQ)_{Cl}$ values for Li^6Cl^{35} can be represented by the equation

$$(eqQ)=eq^0Q+(eq^vQ)_1(v+\tfrac{1}{2})+(eq^vQ)_2(v+\tfrac{1}{2})^2,$$

where $eq^0Q=-2873.2$ kc/sec, $(eq^vQ)_1=-386.6$ kc/sec, and $(eq^vQ)_2=-5.25$ kc/sec. In this expression eq^0Q is the quadrupole interaction constant in the absence of rotation or vibration. The present observations are the first for which it has been necessary to assume a nonlinear variation of (eqQ) with vibration. The linear approximation has been used for the analysis of magnetic resonance data.[41] Duchesne[42] has suggested that variations in halogen interaction constants with vibration are due primarily to changes in the small fraction of covalent character of the alkali-halogen bonds, and assumes that the covalent character increases with internuclear distance. $(eq^vQ)_1$ is then predicted to be negative, which agrees with all the alkali-chloride observations.

The ratios $(eqQ)_{Cl^{35}}/(eqQ)_{Cl^{37}}$ are given in Table V for the first three vibrational states. All of the ratios agree with the much more precise determinations made by Wang *et al.*[43]

The spin-rotation interaction has been interpreted as an interaction of the nuclear magnetic moment with a magnetic field at the nucleus parallel to the axis of

[35] Reference 33, p. 190, Eq. (24).
[36] Lee, Carlson, Fabricand, and Rabi, Phys. Rev. **85**, 607 (1952).
[37] Carlson, Lee, Fabricand, and Rabi, Phys. Rev. **85**, 784 (1952).
[38] J. W. Trischka and R. Braunstein, Phys. Rev. **96**, 968 (1954).
[39] C. H. Townes and B. P. Dailey, J. Chem. Phys. **17**, 782 (1949).
[40] D. R. Inglis, Revs. Modern Phys. **25**, 390 (1953).
[41] H. J. Zeiger and D. I. Bolef, Phys. Rev. **85**, 788 (1952).
[42] J. Duchesne, J. Chem. Phys. **20**, 1804 (1952).
[43] Wang, Townes, Schawlow, and Holden, Phys. Rev. **86**, 809 (1952).

molecular rotation. The magnetic field at the Cl nucleus, H_R was calculated for each vibrational state and isotopic species from the measured c_{Cl} values and the Cl nuclear magnetic moments. All the values agreed within the experimental error. The maximum variation of H_R between the zeroth and third vibrational states consistent with the c_{Cl} values is $\pm 18\%$. For Li^6Cl^{35} in the zeroth vibrational state, $H_R = 4.96 \pm 0.23$ gauss. This value is 54% as great as the value found for Li^6F^{19}.[44] This is the first determination of an H_R ratio for two molecules with the same alkali nucleus. Wick[45] and Foley[46] have discussed possible origins of H_R and the influence of electronic structure on its magnitude. Both theories predict that H_R should be proportional to $1/A$, among other factors. The ratio $A(Li^6F^{19})/A(Li^6Cl^{35})$, calculated[47] as 0.51, agrees well with the observed H_R ratio.

The value of μA obtained from the state identification study was used with the value of $\mu^2 A$ for Li^6Cl^{35} in the zeroth vibrational state to calculate $\mu = 5.9$ Debye units and $r = 2.4$ A. The probable errors in these results are ± 1.3 Debye units and ± 0.4 A, respectively. The value of μ is 18% greater than that calculated by Rittner,[20] but agrees within the experimental error, while the value of r is 21% greater and disagrees slightly with his value.

The ratios $\mu^2 A(Li^6Cl^{35})/\mu^2 A(Li^6Cl^{37})$ are given in Table V for the zeroth, first, and second vibrational states. All of these ratios agree with the ratio of the reduced masses.

Figure 9 shows the linear relation between the vibrational quantum number and the logarithm of the relative intensities of the highest frequency lines in the strong-intermediate field Li^6Cl^{35} spectrum. The vibrational constant, ω_e, was calculated from the slope of this line and the oven temperature, 805°K, to be 536 ± 60 cm^{-1}. The error is based on the estimated error in the oven temperature measurement. The observed value is 32% less than the value calculated by Rittner.[20] For LiI, the experimental value is 31% less than the theoretical value, and in this case Rittner has suggested that the discrepancy is caused by the failure of the polarized-ion model.

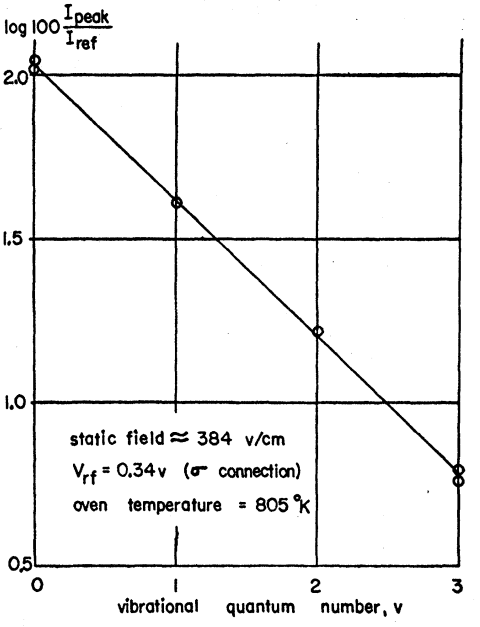

FIG. 9. Linear relationship between the logarithm of the relative intensities of the highest frequency lines in the strong-intermediate field spectra of Li^6Cl^{35}, and the vibrational quantum number. The slope of this curve gives ω_e.

ACKNOWLEDGMENTS

The authors wish to thank Professor P. G. Bergmann and Professor M. Lax for helpful discussions of the radio-frequency Stark effect problem, Mr. C. H. Johnson for care in construction of the secondary emission multiplier, and Mr. S. O. Kastner and Mr. Peter Bratt for their help in the laboratory.

[44] J. C. Swartz and J. W. Trischka, Phys. Rev. 88, 1085 (1952).
[45] G. C. Wick, Phys. Rev. 73, 51 (1948).
[46] H. J. Foley, Phys. Rev. 72, 504 (1947).
[47] The internuclear distance given in reference 9 was used for LiF, and the theoretical value given in reference 20 was used for LiCl.